

1 **A Wastewater-based Epidemiology tool for COVID-19 Surveillance in Portugal**

2 Sílvia Monteiro^{a,*}, Daniela Rente^a, Mónica V. Cunha^{b,c}, Manuel Carmo Gomes^d, Tiago
3 A. Marques^{e,f}, Artur B. Lourenço^b, Eugénia Cardoso^g, Pedro Álvaro^g, Marco Silva^h,
4 Norberta Coelho^h, João Vilaçaⁱ, Fátima Meirelesⁱ, Nuno Brôco^j, Marta Carvalho,
5 Ricardo Santos^a

6

7 ^a Laboratório de Análises, Instituto Superior Técnico, Universidade de Lisboa, Lisbon,
8 Portugal

9 ^b Centre for Ecology, Evolution and Environmental Changes (cE3c), Faculdade de
10 Ciências, Universidade de Lisboa, 1749-016 Lisboa, Portugal.

11 ^c Biosystems & Integrative Sciences Institute (BioISI), Faculdade de Ciências,
12 Universidade de Lisboa, 1749-016 Lisboa, Portugal.

13 ^d Departamento de Biologia Vegetal, Faculdade de Ciências, Universidade de Lisboa,
14 1749-016 Lisboa, Portugal.

15 ^e Centre for Research into Ecological and Environmental Modelling, The Observatory,
16 University of St Andrews, St Andrews, KY16 9LZ, Scotland.

17 ^f Centro de Estatística e Aplicações, Departamento de Biologia Ambiental, Faculdade
18 de Ciências, Universidade de Lisboa, 1749-016, Lisboa, Portugal.

19 ^g Águas do Tejo Atlântico, Fábrica de Águas de Alcântara, Avenida de Ceuta, 1300-
20 254 Lisboa, Portugal.

21 ^h Águas do Norte, Lugar de Gaído, 4755-045 Barcelos, Portugal

22 ⁱ SIMDOURO, ETAR de Gaia Litoral, 4400-356 Canidelo, Portugal

* Corresponding author.

E-mail address: silvia.monteiro@tecnico.ulisboa.pt

- 23 i AdP VALOR, Serviços Ambientais, S.A., Rua Visconde de Seabra, 3, 1700-421
- 24 Lisboa, Portugal

25 **Abstract**

26 The presence of severe acute respiratory syndrome coronavirus 2 (SARS-CoV-2) in
27 wastewater produced interest in its use for sentinel surveillance at a community level
28 and as a complementary approach to syndromic surveillance. With this work, we set
29 the foundations for wastewater-based epidemiology (WBE) in Portugal by monitoring
30 the trends of SARS-CoV-2 RNA circulation in the community, on a nationwide
31 perspective during different epidemiological phases of the pandemic. The Charité
32 assays (E_Sarbeco, RdRP, and N_Sarbeco) were applied to monitor, over 32-
33 weeks (April to December 2020), the dynamics of SARS-CoV-2 RNA at the inlet of five
34 wastewater treatment plants (WWTP), which together serve more than two million
35 people in Portugal. Raw wastewater from three Coronavirus disease 2019 (COVID-
36 19) reference hospitals was also analyzed during this period. In total, more than 600
37 samples were tested.

38 For the first weeks, detection of SARS-CoV-2 RNA was sporadic, with concentrations
39 varying from 10^3 to 10^5 genome copies per liter (GC/L). Prevalence of SARS-CoV-2
40 RNA increased steeply by the end of May into late June, mainly in Lisboa e Vale do
41 Tejo region (LVT), during the reopening phase. After the summer, with the reopening
42 of schools in mid-September and return to partial face-to-face work, a pronounced
43 increase of SARS-CoV-2 RNA in wastewater was detected. In the LVT area, SARS-
44 CoV-2 RNA load agreed with reported trends in hotspots of infection. Synchrony
45 between trends of SARS-CoV-2 RNA in raw wastewater and daily new COVID-19
46 cases highlights the value of WBE as a surveillance tool, particularly after the phasing
47 out of the epidemiological curve and when hotspots of disease re-emerge in the
48 population which might be difficult to spot based solely on syndromic surveillance and

49 contact tracing. This is the first study crossing several epidemiological stages
50 highlighting the long-term use of WBE for SARS-CoV-2.

51

52

53 Keywords:

54 SARS-CoV-2; wastewater-based epidemiology; COVID-19; hospital wastewater

55

56 1. Introduction

57 Climate change, deforestation and population growth led to an increase in contact
58 between humans and wildlife, which may cause interspecies transmission of infectious
59 agents. Such conditions possibly resulted in the occurrence of previous outbreaks
60 including the severe acute respiratory syndrome (SARS; 2002-2004) and the Middle
61 East respiratory syndrome (MERS; 2012-present) outbreaks, all caused by
62 coronavirus (CoV; SARS-CoV and MERS-CoV, respectively). Several authors that
63 have addressed the environmental circulation of viruses had already highlighted the
64 possible occurrence of a new pandemic caused by coronavirus (Wigginton and
65 Ellenberg, 2015; Santos and Monteiro, 2013).

66 Coronavirus disease 2019 (COVID-19) is caused by the severe acute respiratory
67 syndrome coronavirus 2 (SARS-CoV-2), an enveloped, single-stranded RNA virus
68 with a high infection rate. The first clinical cases in Portugal were reported on March
69 2, 2020, with the exponential phase having been reached on March 14, 2020 (RTP,
70 2020). The Portuguese government closed schools on March 16, 2020, and declared
71 the emergency state on March 19, 2020, with the country's entry into the first national
72 lockdown that lasted until May 2, 2020. Reopening occurred in three stages throughout
73 the month of May, with full reopening in June 2020 except for schools that remained
74 closed until the end of the academic year. In September, schools reopened, and partial
75 face-to-face work returned, a steep increase in the number of cases was registered
76 (DGS, 2020). As of December 2, 2020, 307,618 COVID-19 cases had been reported
77 in Portugal, with 4,724 deaths and 229,018 recovered patients (DGS, 2020).

78 Although COVID-19 clinical tests have been developed in record time, the disease
79 spread, and community infection burden often outpaced the capacity for clinical
80 testing. In addition, syndromic surveillance strongly depends on individual reporting

81 and seriousness of clinical symptoms, and how this coincides with diseases known to
82 circulate in the community (Mandi *et al.*, 2020). Rapid approaches to determine the
83 extent of virus spread in the population, ideally in near real-time, are thus needed to
84 slow down transmission.

85 Wastewater-based epidemiology (WBE) has been applied since 2005 to trace
86 pharmaceutical and illicit drug use in the community (Zuccato *et al.*, 2005; Reddy,
87 2010; Singer *et al.*, 2013; Choi *et al.*, 2018). The usefulness and potential of
88 wastewater as a surveillance system for pathogens has already been shown, namely
89 under the global polio eradication initiative, the most successful example of
90 environmental surveillance to date (Hovi *et al.*, 2012; WHO, 2015; Koopmans *et al.*,
91 2017).

92 Several advantages are associated with WBE; firstly, testing wastewater means
93 testing thousands of potentially infected individuals at the same time, and with the
94 potential to identify hotspots of infection prior to syndromic surveillance. Secondly,
95 WBE can highlight trends in viruses shedding over time from symptomatic but also
96 from asymptomatic, pre-symptomatic and post-symptomatic individuals.

97 Although transmitted mainly via respiratory droplets (Meselson, 2020), SARS-CoV-2
98 has been detected in the feces and urine of infected patients, regardless of disease
99 severity or development of gastrointestinal illness (He *et al.*, 2020; Pan *et al.*, 2020;
100 Wölfel *et al.*, 2020; Young *et al.*, 2020). There is little indication that the viruses shed
101 in the stools of infected patients, and therefore circulating in wastewater, are infectious
102 (Wölfel *et al.*, 2020; Zang *et al.*, 2020). Even so, the presence of SARS-CoV-2 RNA in
103 raw wastewater provides valuable information regarding the emergence, prevalence,
104 epidemiology and decrease of SARS-CoV-2 presence in the community, helping the
105 early identification of hotspots of infection.

106 To date, several authors reported the occurrence of SARS-CoV-2 RNA in wastewater
107 samples (Ahmed *et al.*, 2020; Medema *et al.*, 2020; Randazzo *et al.*, 2020; Sherchan
108 *et al.*, 2020) demonstrating the usefulness of WBE for SARS-CoV-2. Several iterations
109 of the application of WBE for SARS-CoV-2 are currently implemented in many
110 countries, such as the Netherlands, Scotland, and Spain among others. The European
111 Commission (EC) has issued a recommendation for surveillance of SARS-CoV-2 and
112 its variants in wastewater as a complementary and independent approach to clinical
113 surveillance, and the member states that choose to accept the recommendation are
114 expected to begin sampling and analysis in October 2021, with the results being
115 reported directly to the EC (EC, 2021).

116 In this study, we report for the first time the results of SARS-CoV-2 RNA monitoring in
117 raw wastewater in Portugal, in a study covering about 20% of the Portuguese
118 population, corresponding to more than two million people, over a 32-weeks period.
119 More than 600 samples were collected from five wastewater treatment plants (WWTP)
120 and three COVID-19 hospitals in two regions of the country: a north cluster (four
121 municipalities) and a south cluster in Lisboa e Vale do Tejo (LVT) (six municipalities).
122 To the best of our knowledge, this is the first study jointly evaluating the presence of
123 SARS-CoV-2 RNA in raw wastewater from WWTP and COVID-19 hospitals.
124 Altogether, in contrast with the already published studies that only looked at the early
125 stages of the pandemic, and by encompassing several distinct epidemiological stages
126 of this disease, this study demonstrates the long-term usefulness of using WBE for
127 SARS-CoV-2 and potential long-term application to future health crisis.

128 2. Materials and Methods

129 2.1. Clinical surveillance data

130 Clinical surveillance data were obtained from the Reports from the Portuguese Health
131 Authority (DGS, 2020). Data from clinical surveillance for each municipality were
132 presented daily in the reports from the Health Authority, being provided on a weekly
133 basis after July 2020.

134

135 2.2. Porcine epidemic diarrhea virus (PEDV) strain and cell lines

136 Porcine epidemic diarrhea virus (PEDV) strain CV777 (kindly provided by Dr. Gloria
137 Sanchez, IATA-CSIC) is an enveloped virus from the genus *Alphacoronavirus* and
138 member of the *Coronaviridae* family, responsible for the porcine epidemic diarrhea.
139 PEDV was propagated in Vero cell line (ATCC CCL-81, LGC Standards). Briefly, Vero
140 cells were grown in Dulbecco's Modified Eagle's Medium (DMEM; Gibco),
141 supplemented with 100 units/mL of penicillin (Lonza), 100 units/mL of streptomycin
142 (Lonza), and 10% heat-inactivated fetal bovine serum (Biological Industries). Cells
143 were cultured in T175 flasks at 37 (\pm 1) °C under 5 % CO₂. For infection with PEDV,
144 cells were grown in T25 flasks and inoculated with 100 μ L of viral stock. At 2h post
145 infection, DMEM supplemented with 0.3% tryptose phosphate broth, 100 units/mL of
146 penicillin (Lonza), 100 units/mL of streptomycin (Lonza), and 10 μ g/ μ L trypsin, was
147 added to the flasks. Flasks were then incubated at 37 (\pm 1) °C in 5% CO₂ for 4 days.
148 PEDV were recovered following three cycles of freeze/thawing and centrifugation at
149 1,100 xg for 10 min. Quantification was performed by RT-dPCR as described on
150 section 2.5 using the primers and probes from Table 1 (Zhou *et al.*, 2017), following
151 nucleic acid extraction as described on section 2.4. After absolute quantification by
152 RT-dPCR (as described below), a stock solution was prepared in DNase/RNase free

153 water to obtain a PEDV final concentration of 1.21×10^4 GC/L in wastewater. The
154 same stock was used in all experiments described below.

155

156 2.3. Absolute quantification by RT-dPCR

157 RT-dPCR was used to determine the exact concentration of PEDV. PEDV was
158 amplified using the AgPath-ID One-Step RT-PCR kit (Thermo Fischer Scientific) with
159 the set of primers and probes described on Table 1 (Zhou *et al.*, 2017). The 15 μ L
160 reaction mixture consisted of 7.5 μ L of 2 \times RT-PCR buffer, 0.6 μ L of 25 \times RT-PCR
161 enzyme mix, 800 nM of each primer, 200 nM of probe, 3.63 μ L RNase/DNase-free
162 water, and 3 μ L of DNA (diluted 4-, 5-, 6- fold). The reaction mixture was then spread
163 over the QuantStudio 3D Digital PCR chip (Thermo Fischer Scientific) and the chips
164 transferred to the QuantStudio 3D Digital PCR thermal cycler. Amplification was
165 performed as follows: PEDV: 10 min at 45 $^{\circ}$ C, 10 min at 96 $^{\circ}$ C, 39 cycles of 2 min at
166 60 $^{\circ}$ C and 30 s at 98 $^{\circ}$ C, and a final elongation step for 2 min at 60 $^{\circ}$ C. Reactions were
167 performed in duplicate, and a non-template control (NTC) was included in each run.

168

169

170 2.4. Sampling sites and sample collection

171 Raw wastewater samples ($n = 404$) were collected between April 27, 2020, and
172 December 2, 2020, from five WWTP located in the North (Gaia Litoral (GA) and
173 Serzedelo II (SE)) and in LVT (Alcântara (AL), Beirolas (BE), and Guia (GU)) (Fig. S1)
174 of Portugal. Further information about these WWTP catchments is provided in Table
175 S1. Sampling took place for 102 days, covering 220 of calendar days in total.

176 Raw wastewater from three reference COVID-19 hospitals (Hospital Curry Cabral
177 (HCC), Lisbon; Hospital Sra. Oliveira (HSO), Guimarães (North); and Hospital Santos

178 Silva (HSS), Vila Gaia (North); $n = 204$), in the catchment area of the WWTP, was also
179 sampled.

180 Twenty-four-hour composite samples were collected using automated samplers
181 (ISCO, US), except for HSO and HSS, where due to logistical issues only grab
182 samples were taken. Samples were transported refrigerated to the laboratory, within
183 8 h of collection and processed immediately upon arrival to the laboratory.

184

185 2.5. Processing of raw wastewater

186 Upon arrival to the laboratory, 1-L of raw wastewater from WWTP and COVID-19
187 hospitals was concentrated using hollow-fiber filters Inuvai R180 (molecular weight
188 cut-off ≤ 18.8 kDa; Inuvai, a division of Fresenius Medical Care, Germany). A stock of
189 PEDV was added to the samples to a final concentration of 1.21×10^4 GC/L (quantified
190 as described above). Samples were eluted in 300 mL of 1X PBS containing 0.01%
191 sodium polyphosphate (NaPP) and 0.01 Tween 80/0.001% antifoam and precipitated
192 overnight with 20% polyethylene glycol (PEG) 8000. Samples were then centrifuged
193 at 10000 $\times g$ for 30 min and resuspended in 5 mL 1X PBS, pH 7.4 (Blanco *et al.*, 2019).
194 Samples were kept at (-80 ± 10) °C until further processing. Recovery efficiency varied
195 between 40 and 82%, at an average of 61% (± 16).

196

197 2.6. Viral RNA extraction, detection, and quantification

198 Viral RNA was extracted from 220 μ L of concentrated samples using the QIAamp
199 FAST DNA Stool Mini kit (QIAGEN, Germany), according to the manufacturer's
200 instructions. The RNA was recovered in a final volume of 100 μ L.

201 Primers and probes used in this study are presented in Table 1. The recovery
202 efficiency for RNA extraction was performed using murine norovirus (MNV), which was

203 added to the concentrates as an extraction control. MNV RNA was detected and
204 quantified using the assay described by Baert *et al.*, 2008. SARS-CoV-2 RNA was
205 detected using the Charité assays: the E_Sarbeco, targeting the envelope protein
206 gene, the RdRp that targets the RNA-dependent RNA polymerase gene and the
207 N_Sarbeco, which targets the nucleoprotein (Corman *et al.*, 2020).

208 One-step RT-qPCR assays (AgPath-ID™ One-Step RT-PCR, Thermo Scientific,
209 USA) was used for the quantitative detection of SARS-CoV-2, PEDV, and MNV. For
210 the specific detection and quantification of viral RNA, 5 µL of 4-fold and 10-fold
211 dilutions of each viral RNA extract were also assayed in parallel with crude extracts;
212 dilutions were meant to overcome amplification inhibition due to the complex nature of
213 the samples. Cycle Threshold differences (ΔCt) ≥ 2.50 and 3.50 between crude
214 extracts and 4-fold and 10-fold dilutions, respectively, were considered amplification
215 inhibition free.

216 The final volume of reaction mixture was 25 µL, composed of 800 nM of each primer,
217 200 nM of probe and 5 µL of extracted RNA. RT-qPCR reactions were carried out at
218 45 °C for 10 min, 95 °C for 10 min, followed by 45 cycles of amplification at 95 °C for
219 15 s and 58 °C for 45 s for SARS-CoV-2 and 60 °C for 45 s for PEDV and MNV. RT-
220 qPCR was performed on an Applied Biosystems 7300 Real-Time PCR System
221 (Applied Biosystems, US). Reactions were considered positive only if the cycle
222 threshold was below 40 cycles (Medema *et al.*, 2020; F. Wu *et al.*, 2020). Quantification
223 of E_Sarbeco and RdRp assays was performed through calibration curves using 10-
224 fold dilutions of nCoV-ALL-Control plasmid (Eurofins Genomics, Germany), ranging
225 from 1.94 to 1.94×10^6 and 1.00 to 1.00×10^6 GC per reaction respectively.
226 Quantification of N_Sarbeco assay was performed using 2-fold and 10-fold dilutions
227 (ranging between 2.00 to 2.00×10^4 GC per reaction) of the Amplirun SARS-CoV-2

228 RNA control (Vircell, Spain). Negative controls (extraction and RT-qPCR assay) were
 229 also performed using DNase/RNase free distilled water, following the same conditions
 230 as the samples. The extraction efficiency using MNV as proxy averaged 70% ($\pm 19\%$).

231

232 **Table 1.**

233 Primers and probes used in this study

Assay	Sequence (5' - 3') ^a	Length (bp)	Location in SARS-CoV-2 genome (bp)
MNV	F: CACGCCACCGATCTGTTCTG R: GCGCTGCGCCATCACTC P: 6FAM-CGCTTTGGAACAATG-MGB	108	4,972 – 5,080
PEDV	F: CAGGACACATTCTTGGTGGTCTT R: CAAGCAATGTACCACTAAGGAGTGTT P: FAM-ACGCGCTTCTCACTAC-MGB	140	26,010 - 26,149
SARS-CoV-2: E_Sarbeco	F: ACAGGTACGTTAATAGTTAATAGCGT R: ATATTGCAGCAGTACGCACACA P: 6FAM-ACACTAGCCATCCTTACTGCGCTTCG-BHQ	112	26,141 – 26,253
SARS-CoV-2: RdRp	F: GTGARATGGTCATGTGTGGCGG R: CARATGTTAAASACACTATTAGCATA P1: 6FAM-CCAGGTGGWACRTCATCMGGTGATGC-BHQ P2: 6FAM-CAGGTGGAACCTCATCAGGAGATGC-BHQ	99	15,361 – 15,460
SARS-CoV-2: N_Sarbeco	F: CACATTGGCACCCGCAATC R: GAGGAACGAGAAGAGGCTTG P: 6FAM-ACTTCCTCAAGGAACAACATTGCCA-BHQ	127	28,555 – 28,682

234 ^a W is A/T; R is G/A; M is A/C; S is G/C. FAM: 6-carboxyfluorescein; MGB: minor groove binder; BHQ: blackhole
 235 quencher.

236

237 2.7. SARS-CoV-2 RNA load estimates standardized to population

238 Standardization of SARS-CoV-2 RNA concentration to population and WWTP for each
 239 sampling date was performed in accordance with Eq. 1 (Gonzalez *et al.*, 2020). For
 240 this calculation only the results from E_Sarbeco assay were used since it was the
 241 most sensitive assay.

242

243
$$L_{WWTP} = \frac{C_{WWTP} \times V \times f}{P}$$

244 where:

245 L_{WWTP} is SARS-CoV-2 RNA load in the WWTP standardized to the population (GC per
246 person per day in the catchment)

247 C_{WWTP} is the SARS-CoV-2 RNA concentration in samples yielded by the E_Sarbecco
248 assay (GC/L)

249 V is the average daily flow of wastewater in the WWTP during the sampling day
250 (m^3/day)

251 f is the conversion factor between L and m^3

252 P is the estimated population within the WWTP catchment.

253

254 2.8. Data analysis

255 All data analysis was done with SPSS version 26 (IBM Corporation, US). For statistical
256 analysis, all RT-qPCR below the limit of detection (LOD) were substituted by the LOD
257 with subsequent \log_{10} transformation. The LOD was 3.99, 5.52 and 5.74 GC per
258 reaction for E_Sarbecco, RdRp and N_Sarbecco assays, respectively. Kruskal-Wallis
259 test (KW statistics) was conducted to compare differences in the total number of
260 SARS-CoV-2 RNA detection for each assay, and pairwise comparison was performed
261 with Dunn's test. Mann-Whitney test was used to determine the impact of sampling
262 type (composite *versus* grab samples collected at hospitals). Spearman rank order
263 correlation was used for calculation of correlation coefficients between the
264 concentrations of SARS-CoV-2 RNA obtained by the three assays and between the
265 number of hospitalized COVID-19 patients and the concentration of SARS-CoV-2 RNA
266 at each hospital.

267

268 3. Results and Discussion

269 3.1. Performance of Charité assays on SARS-CoV-2 quantification in 270 wastewater

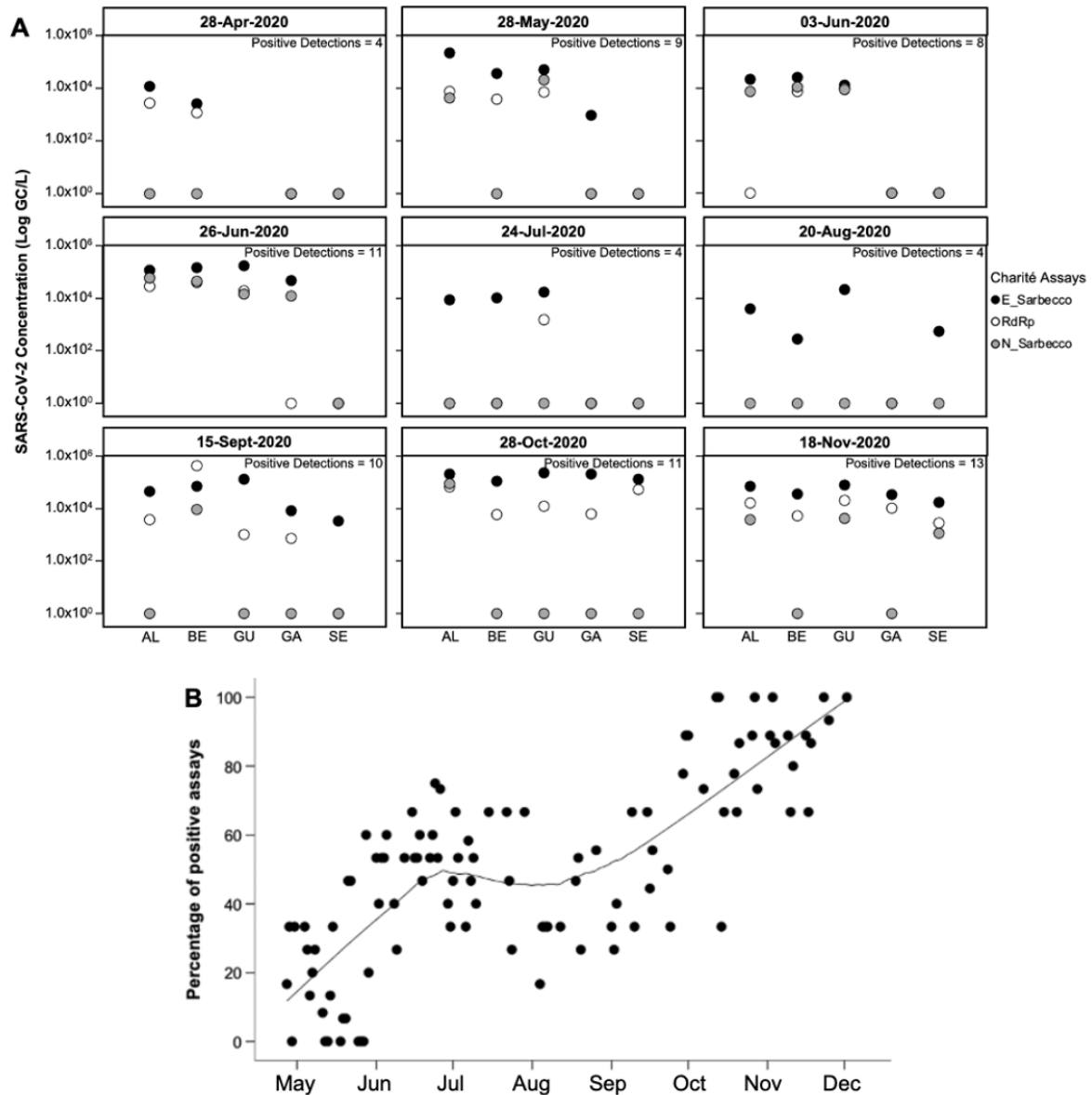
271 The first RT-qPCR assays for the detection of SARS-CoV-2 were designed at the
272 beginning of the pandemic following the disclosure of the first SARS-CoV-2 sequence,
273 the designated Charité assays: E_Sarbecco, RdRp (P1 and P2) and N_Sarbecco
274 (Corman *et al.*, 2020). Environmental studies generally rely on the use of a single
275 assay to determine the presence of a target (La Rosa and Muscillo, 2013). However,
276 due to sensitivity and specificity issues, WBE studies for SARS-CoV-2 have included
277 multiple gene targets, including the Charité (Wurtzer *et al.*, 2020; Medema *et al.*, 2020;
278 Chavarria-Miró *et al.*, 2020) and the CDC assays (Ahmed *et al.*, 2020; Medema *et al.*,
279 2020; Randazzo *et al.*, 2020). In the 32-week study reported here, the three assays
280 were compared with respect to detection rates and concentrations to determine the
281 need to run all three assays in future WBE studies.

282 Detections of SARS-CoV-2 RNA were scarcer during the lockdown and reopening
283 months (April-May), with discrepant results among the assays (Fig. 1A). The results
284 of SARS-CoV-2 RNA prevalence for the three assays ($n = 404$), including below and
285 above LOD, coincided in 193 samples. This number dropped to 80 samples when
286 considering just samples above the LoD. In 116 samples, detection occurred for two
287 assays and in 95 samples only one assay was detected.

288 Agreement between assays increased and became more consistent as the total
289 number of detections increased, particularly following the end of the lockdown (Fig.
290 1A, B). The E_Sarbecco assay was detected more frequently, with consistent
291 detections over the 32-week period of sampling. A total of 290, 177, and 100 samples
292 tested positive for E_Sarbecco, RdRp, and N_Sarbecco, respectively. The detection

293 rates for all assays showed statistically significant differences (KW = 181.45, degrees
294 of freedom = 2, $p < 0.001$). This result is in line with the original publication that indicated
295 that E_Sarbeco and RdRp assays were more sensitive than N_Sarbeco assay
296 (Corman *et al.*, 2020). There was also statistical difference in the number of detections
297 in the pair-wise comparison between individual assays ($p < 0.001$, for all assays). The
298 number of detections for N_Sarbeco assay was significantly lower than for the other
299 two assays, possibly due to the higher limit of detection determined for this assay or
300 possible loss of RNA integrity (Philo *et al.*, 2020).

301



302

303 **Fig. 1.** SARS-CoV-2 RNA concentration estimated with Charité assays in selected sampling dates. The
 304 concentrations in each WWTP, in selected sampling dates, are depicted on the x axis of the figure. The dates were
 305 chosen at (roughly) monthly intervals, starting from April 28, with exception of June 3, which was added because
 306 it represented one of the first dates following the complete reopening of the country (A); epidemiological phase
 307 (EPI) I: emergency state; EPI II: calamity state; EPI III: contingency and alert state; EPI IV: emergency state.
 308 Percentage of positive detection assays across the study period. Obtained with the 3 Charité assays. The trendline
 309 was drawn with LOWESS smoothing (B).

310

311

312 The positivity rates for RdRp and N_Sarbeco assays increased with increasing
 313 concentrations yielded by the E_Sarbeco assay. At concentrations between 10^2 and
 314 10^4 GC/L, the positivity rate was 20% and 6% for the RdRp and N_Sarbeco assays,

315 respectively. For E_Sarbeco assay concentrations above 10^4 GC/L, the positivity
316 rates increased to 77% for the RdRp assay and 45% for the N_Sarbeco assay (Fig.
317 S2).

318 The concentration of N_Sarbeco *versus* the other two assays in raw wastewater
319 showed only moderate correlation (Spearman rank order correlation $r = 0.50$ for
320 N_Sarbeco vs. RdRp; $r = 0.56$ for N_Sarbeco vs E_Sarbeco; $p < 0.01$, $n = 404$). The
321 correlation between E_Sarbeco and RdRp concentration was significant ($r = 0.74$,
322 $p < 0.01$, $n = 404$) (Fig. S3). Such figure facilitates the comparison of the distribution of
323 positive and negative results for each pair of assays.

324 The discrepancies observed amongst E_Sarbeco, RdRp and N_Sarbeco assays
325 agreed with previous reports, not only using the Charité assays but also the CDC
326 protocol (Chavarria-Miró *et al.*, 2020; Corman *et al.*, 2020; Medema *et al.*, 2020;
327 Randazzo *et al.*, 2020; Westhaus *et al.*, 2020).

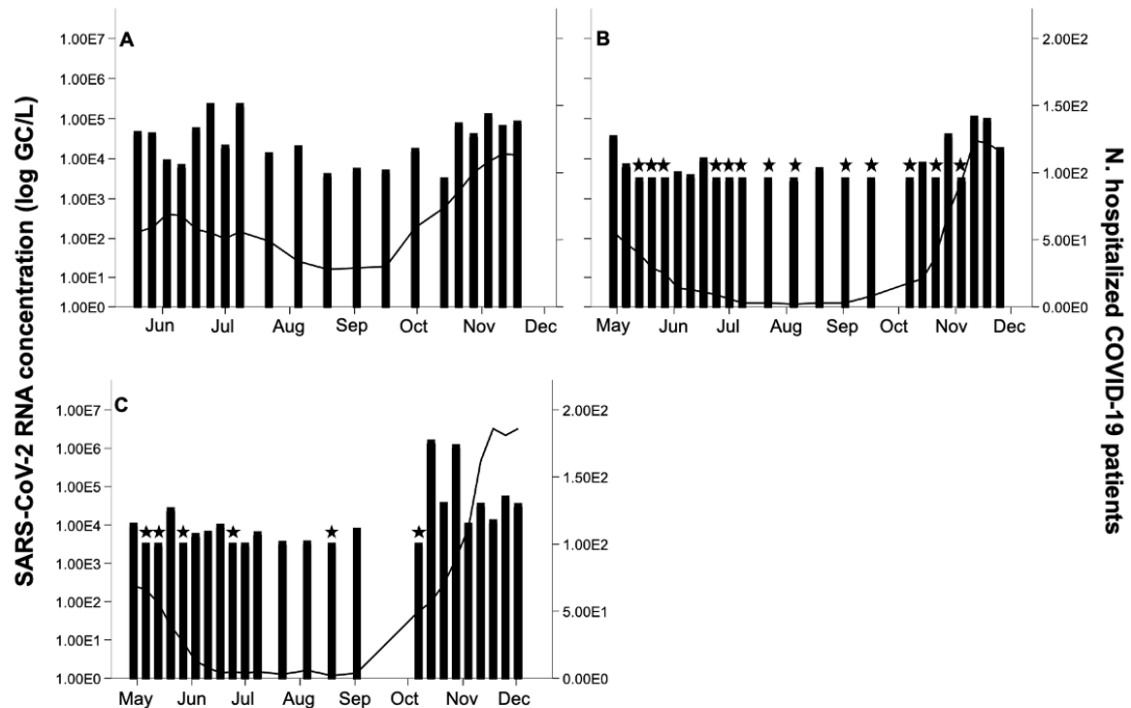
328

329 3.2. Detection of SARS-CoV-2 RNA in hospital wastewater samples

330 A total of 204 COVID-19 hospital wastewaters have been sampled in the 32-week
331 study period and evaluated for the presence of SARS-CoV-2 RNA. Ninety-seven
332 samples were positive for at least one SARS-CoV-2 assay (97/204; 48%), at
333 concentrations ranging from 10^3 to 10^6 GC/L (Fig. S4). The percentage of positive
334 samples varied from 24% (HSS) to 85% (HCC). The Cq values varied between 26.36
335 and 38.43 for the E_Sarbeco assay, with agreement in detection for the three assays
336 in 62% of the samples (including samples below the LoD) and in 21% of the samples
337 considering just SARS-CoV-2 RNA positive samples ($n = 98$). Although highly
338 relevant, the number of studies reporting the specific detection of this virus in hospital
339 wastewater is very limited (J. Wang *et al.*, 2020; D. Zhang *et al.*, 2020; Gonçalves *et*

340 *al.*, 2021). Although no quantification was made, J. Wang *et al.* (2020) and Gonçalves
341 *et al.* (2021) reported similar Ct values to those obtained in our study. Detection
342 frequency of SARS-CoV-2 RNA in hospital wastewater increased by the end of the
343 study, when the number of cases in Portugal increased steeply and a high number of
344 hospital beds were being occupied by COVID-19 patients (Fig. 2). From the end of the
345 lockdown to schools reopening and return to partial face-to-face work (April through
346 mid-September), the number of hospitalized COVID-19 cases decrease from an
347 average of 60 to 3 in HSS and from 73 to 5 in HSO, increasing to 115 and 162 in
348 November, respectively. As for HCC, the monthly average number of hospitalized
349 COVID-19 cases remained stable from April to July (average ranging between 48 and
350 61 in April and June, respectively), decreasing during the month of August (30) only
351 to increase again in September. By the end of the sampling period, the average
352 number of hospitalized COVID-19 cases in HCC increased to 114.

353



354

355 **Fig. 2.** Gene fragment concentration in hospital wastewater (bars), and the number of hospitalized COVID-19 cases
 356 (line) in the three hospitals. HCC (A); HSS (B); HSO (C). ★ Indicates values below the LoD for E_Sarbeco assay.
 357 Values represented in the figures

358

359

360 Correlation analysis was used to investigate the quantitative relation of SARS-CoV-2

361 RNA concentration to the number of hospitalized COVID-19 cases in each hospital.

362 No correlation was found in HCC and only moderate association was obtained for the

363 other two hospitals (Spearman rank order correlation $r = 0.57$ for HSS and $r = 0.60$ for

364 HSO; all $p < 0.01$). During the phase with lower number of hospitalized COVID-19

365 cases at HSS, most of the samples collected were below the LOD, a similar result to

366 that observed in HSO hospital (Fig. 2). On the other hand, SARS-CoV-2 RNA

367 detection at HCC was consistent throughout the study. Sporadic detection of SARS-

368 CoV-2 RNA during this phase could be attributed not only to the low number of

369 hospitalized COVID-19 patients but also to the different sampling strategy. While HCC

370 samples were composite, grab samples were taken at the other two hospitals.

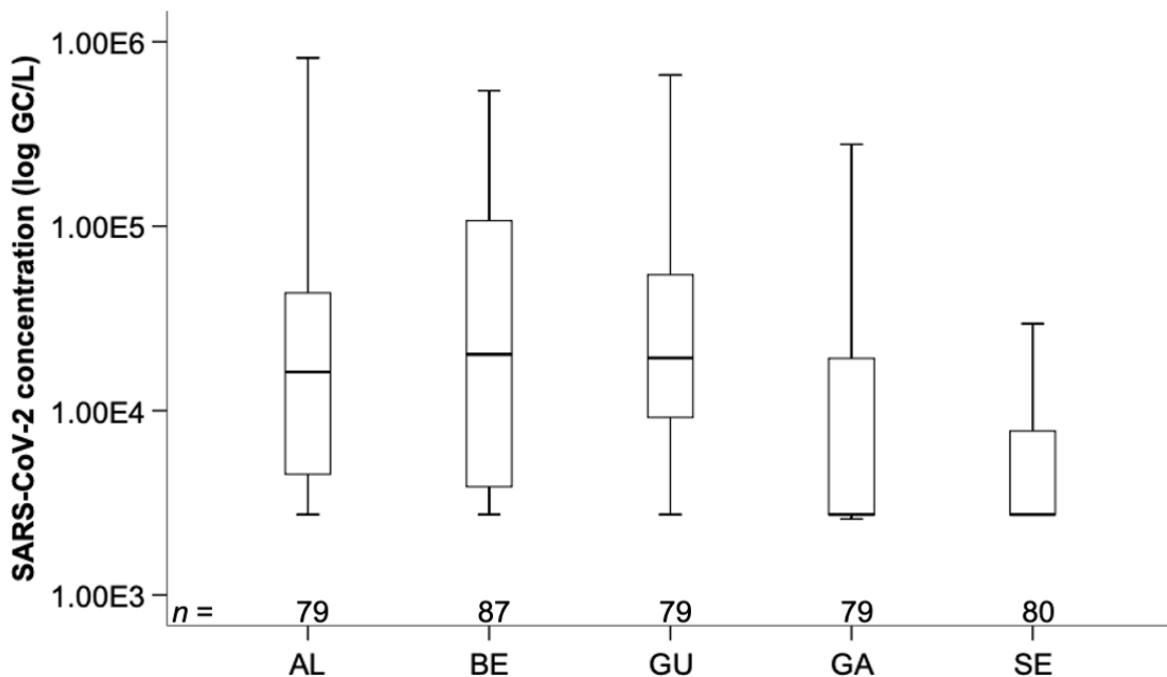
371 Statistically significant differences ($p < 0.001$; Mann-Whitney U test) were determined
372 between composite and grab samples. Composite sampling provides a better
373 representation of a heterogenous sample than grab samples tested separately as the
374 variance between samples decreases and the analytical results reflect more
375 thoroughly the real composition of the sample. Automated systems (composite
376 sampling) are commonly used for chemical analysis of water in industrial and public
377 health applications (U.S. Geological Survey, 2006, 2010; Baird *et al.*, 2017).
378 Composite sampling has also been widely used to analyze trace contaminants such
379 as mycotoxins in food and to determine microbial populations in soil and water (Jarvis,
380 2007; Cornman *et al.*, 2018). However, for quantification purposes, composite
381 sampling has not been routinely applied in microbiological analysis of water due to a
382 possible dilution effect. This paradigm has shifted with SARS-CoV-2, with this
383 respiratory virus being found only in approximately 50% of the stools of infected
384 patients at varying concentrations (10^2 to 10^8 per gram of stool) (Lescure *et al.*, 2020;
385 Pan *et al.*, 2020; Wölfel *et al.*, 2020; Y. Wu *et al.*, 2020; Xu *et al.*, 2020). Even if
386 composite sampling is not paramount in WWTP settings, in single, point locations
387 (such as hospital wastewaters) it may have a deeper impact with the results from this
388 study corroborating the initial hypothesis, as a lower percentage of positive samples
389 were obtained for the hospitals where grab samples were taken.

390

391

392 3.3. Temporal dynamics of SARS-CoV-2 RNA in raw wastewater

393 A total of 404 raw wastewater were collected between April 27 and December 2, 2020
394 and monitored for the presence of SARS-CoV-2 RNA. Concentration in positive
395 samples, for E_Sarbeco assay, varied generally between 10^3 and 10^5 GC/L (Fig. 3).



397

398 **Fig. 3.** SARS-CoV-2 concentration in the tested WWTP. AL- Alcântara; BE – Beirolas; GU – Guia; GA – Gaia
 399 Litoral; SE – Serzedelo. Boxes, 25th and 75th percentile; lines within the boxes, median; whiskers, 10th and 90th
 400 percentile, respectively. *n*, number of samples in each category.

401

402

403 Table 2 shows SARS-CoV-2 RNA concentrations and percentage of positive samples
 404 discriminated by WWTP. The prevalence of SARS-CoV-2 RNA varied between 51%
 405 in SE and 85% in BE and GU, with WWTP located in LVT conveying the highest
 406 number of positive detections.

407

408 **Table 2.**

409 SARS-CoV-2 RNA concentration and percentage of positive samples in the overall study and in each WWTP

Sampling location	% Positive samples	SARS-CoV-2 RNA concentration variation (GC/L)
All WWTP	72 (291/404)	$3.13 \times 10^3 - 8.95 \times 10^5$
AL	82 (65/79)	$3.86 \times 10^3 - 8.17 \times 10^5$
BE	85 (74/87)	$3.13 \times 10^3 - 5.43 \times 10^5$
GU	85 (67/79)	$3.41 \times 10^3 - 8.95 \times 10^5$

GA	56 (44/79)	$3.30 \times 10^3 - 3.93 \times 10^5$
SE	51 (41/80)	$3.29 \times 10^3 - 3.20 \times 10^5$

410

411 The concentrations found in this study are in line with those documented in the US,
412 and The Netherlands (Gonzalez *et al.*, 2020; Medema *et al.*, 2020; Sherchan *et al.*,
413 2020). A study conducted at the early stages of the pandemic in the Metropolitan area
414 of Barcelona has shown concentrations, as determined by the E_Sarbeco assay, in
415 the same range as in our study (Chavarria-Miró *et al.*, 2021). Flood *et al.* (2021) have
416 determined SARS-CoV-2 RNA in raw wastewater at an average concentration of 8.53
417 $\times 10^5$ GC/L, when using the E_Sarbeco assay. Wurtzer *et al.* (2020) detected SARS-
418 CoV-2 RNA, using the E_Sarbeco assay, in concentrations up to approximately 2.5
419 $\times 10^6$ GC/L, with the number of cases reaching the highest number at more than 5000
420 daily cases (ECDC, 2020). Nonetheless, studies developed in Spain documented
421 concentrations at least two orders of magnitude superior to the mean concentrations
422 observed in this study (Randazzo *et al.*, 2020). The differences found between studies
423 may result from a multitude of factors, including disease prevalence, and variability in
424 the workflows including detection assays (Gonzalez *et al.*, 2020).

425

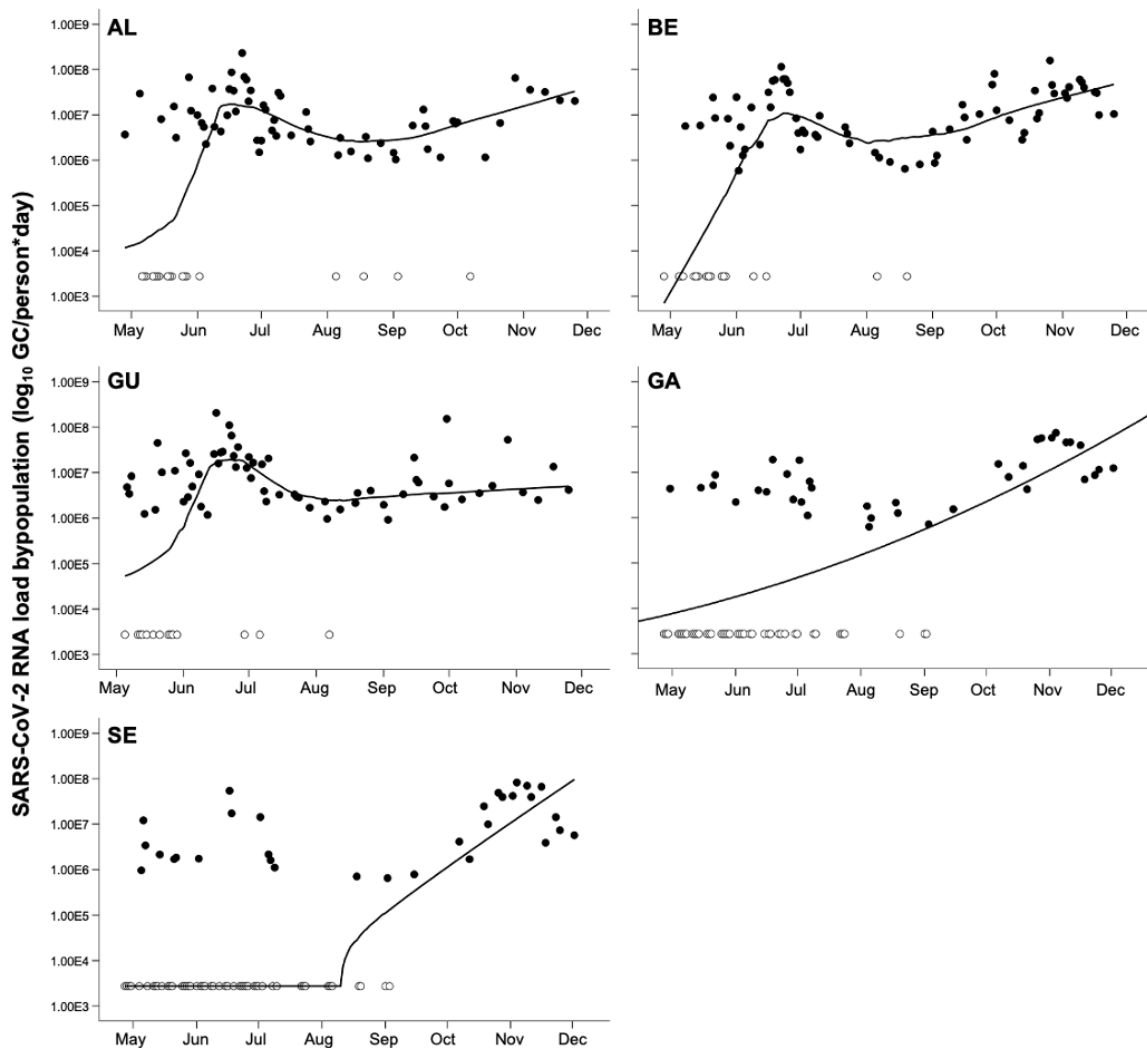
426 3.4. Regional distribution of SARS-CoV-2 RNA concentration

427 This study was conducted over a period of 32-weeks (eight months), comprising the
428 end of lockdown (April) and consecutive reopening stages (May), full reopening with
429 online classes for students and partial face-to-face work (June), the vacation period
430 (July and August), schools reopening and return to partial face-to-face work (mid-
431 September) (Fig. S5). The new number of reported cases decreased sharply from April
432 (mean, 570) to May (mean, 249), increasing again in June (mean, 325), according to
433 Reports from the Portuguese Health Authority (DGS, 2020). The average number of

434 new cases decreased in July (mean, 286) and August (mean, 224) only to increase
435 again in September (mean, 605), October (mean, 2,192) and November (5,058).

436 Fig. 4 shows the load of SARS-CoV-2 RNA, by date, normalized to population in the
437 service area of each WWTP. SARS-CoV-2 RNA detection in WWTP for the LVT region
438 showed lower percentages of detection during April-May, increase in the frequency of
439 detection in June, decrease for the months of July, August and mid-September, and a
440 steep increase from mid-September onwards (Fig. S6). The viral load in the LVT
441 region in this region followed a similar trend to that of the prevalence of the virus.
442 Nonetheless, the detection of SARS-CoV-2 RNA in WWTP from LVT region remained
443 high after the end of lockdown.

444



445

446 **Fig. 4.** SARS-CoV-2 RNA load, by date, normalized to the population in the service area of each WWTP. Black dots indicate samples above the LoD, white dots represent samples below the LoD (with LOWESS smoothing)

447

448

449 SARS-CoV-2 RNA load in the north region of the country (GA and SE) remained stable

450 during the period comprising April to mid-September, sharply increasing afterwards

451 following the trends observed in the syndromic surveillance (Fig. S6). Occasional

452 detections were observed during the lockdown and following periods with a gradual

453 increase in the frequency of detection until mid-September. Upon school reopening,

454 and return to partial face-to-face work, a steep increase occurred in the SARS-CoV-2

455 RNA load in all locations. During pre-lockdown and lockdown, the North region was

456 the most affected by COVID-19, a pattern that shifted following the reopening with the

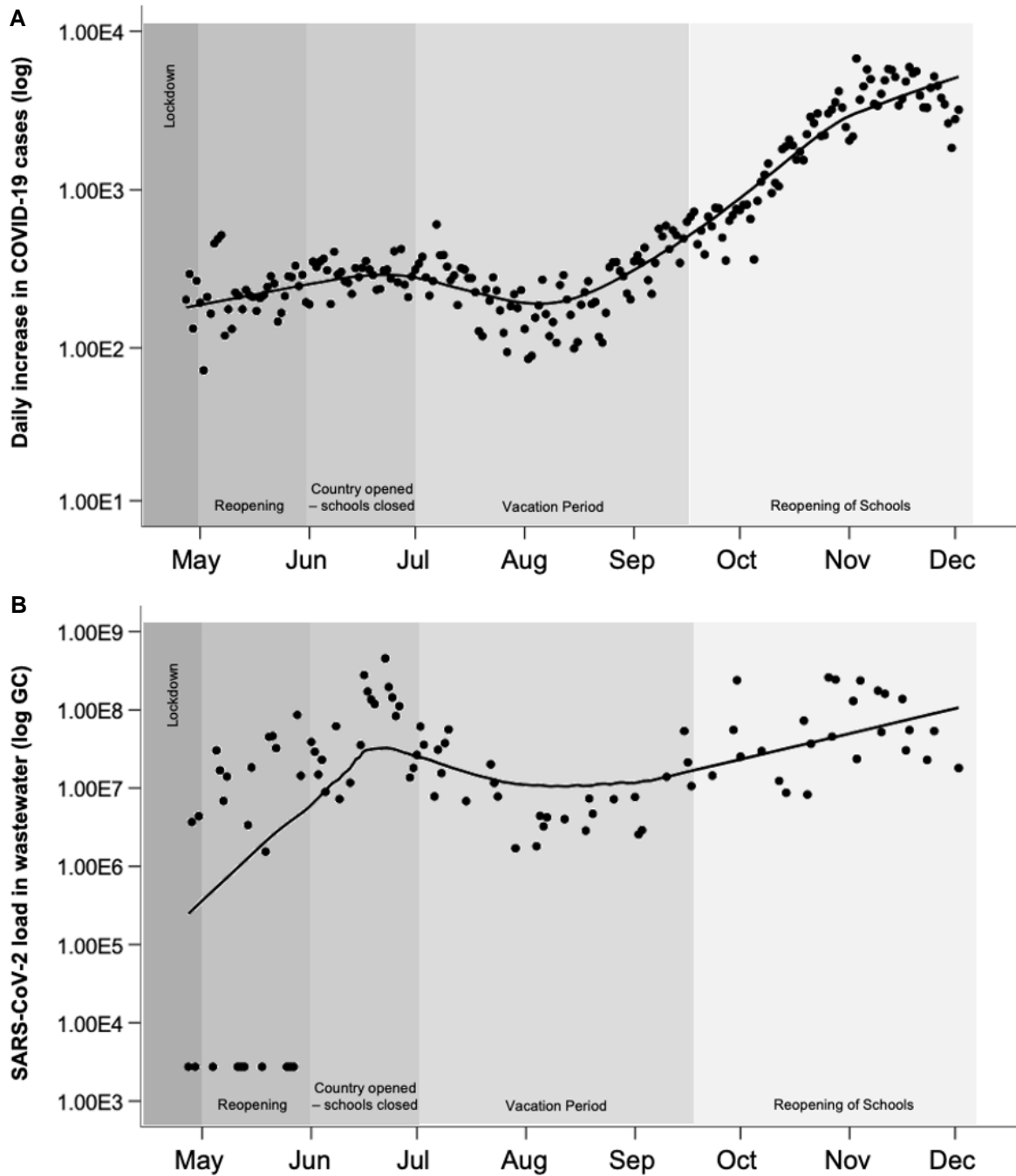
457 great Lisbon area becoming the main contributor to the increase in the number of
458 COVID-19 cases observed throughout May and June (Fig. S7). Altogether, the
459 cumulative number of COVID-19 cases increased at a slow pace from the end of April
460 until the beginning of October, with a noticeable increase at this stage mainly due to
461 the new spike in cases registered in the North region. Overall, and until October 25,
462 2020, Lisbon and Sintra, both in LVT, had the highest number of confirmed COVID-19
463 cases (9,202 and 7,454, respectively), followed by Amadora, Loures, (3,722, and
464 4,164, respectively), also in the LVT region. In the North region, Vila Nova de Gaia
465 had the highest number of confirmed cases (3246).

466 Data from Fig. 4 can be used for comparison with existing outbreaks reported by the
467 health department. For instance, the increase in the detection of SARS-CoV-2 RNA in
468 the BE service area documented during June was likely caused by outbreaks in
469 Sacavém-Prior Velho, Camarate-Unhos-Apelação and Santa Clara civil parishes.
470 Such projection can also show trends in viruses spread over time within localized
471 populations, not only from symptomatic but also from asymptomatic, pre-symptomatic
472 and post-symptomatic. Such representation shows that although the number of
473 clinically tested cases in the population was more consistent, the viral concentration
474 remained mostly heterogeneous with a vast influence from localized hotspots of
475 infection.

476 Fig. 5 illustrates the combined loads of SARS-CoV-2 RNA, over time, in the chosen
477 WWTP service areas. The concentrations of SARS-CoV-2 RNA (E_Sarbeco) from
478 all five WWTP were merged daily to obtain an estimation of the concentrations in the
479 regions tested.

480 The trend combined for the regions was equivalent to the trends observed in the
481 clinical surveillance. It is evident from the present data that the reopening phase, in

482 May, corresponded to an increment in the viral load, which is in accordance with the
483 increase observed, in Portugal, in the number of new daily COVID-19 reported cases.
484 Following this phase, the country entered the summer vacation period, with a slight
485 decrease in viral load. The third and final stage of viral loading, in this study, occurred
486 after the reopening of schools and return to partial face-to-face work. At this stage,
487 viral loading increased gradually in parallel with the rise of new daily COVID-19 cases
488 in the country.
489



490

491 **Fig. 5.** Daily increase in COVID-19 cases (A) (DGS, 2020) and combined SARS-CoV-2 concentration in
 492 wastewater for the regions under study over the 32-week period with LOWESS smoothing (B)

493

494

495 The pattern similarity between the number of new COVID-19 cases reported daily,
 496 provided by clinical testing, and the load of SARS-CoV-2 RNA in raw wastewater
 497 further proves the usefulness of WBE for SARS-CoV-2, as well as potential future

498 pandemic. Such representation (Fig. 5B), could therefore be integrated with syndromic
499 surveillance data, as an early-warning system for the increase of the number of
500 infected individuals within the community. Although the number of cases peaked
501 during the month of November, SARS-CoV-2 RNA loading did not differ acutely
502 between the months of June and October-November, despite the steep difference in
503 the number of cases. This may have resulted from an increase in the testing
504 capacity/availability of tests during the latter phase (Fig. S8). Such result further
505 highlights the usefulness of WBE for SARS-CoV-2, particularly in locations where
506 testing is reduced or even unavailable.

507 Results from individual testing should be the most accurate measure of transmission
508 and disease occurrence in the population, but the scale of testing (spatial and
509 temporal) necessary to have accurate information and to be able to follow the spread
510 of the virus in the population is unrealistic and economically impracticable for most
511 countries. Additionally, continuous testing indispensable for the effective control of the
512 disease is economically and timely challenging. Wastewater monitoring represents
513 testing thousands of infected people simultaneously rather than a single person and
514 is complimentary to syndromic surveillance of COVID-19. The knowledge provided by
515 the analysis of wastewater can, therefore, be employed as an impartial surveillance
516 tool, reflecting more closely the health of a population. Moreover, wastewater may also
517 allow for a precocious detection of new SARS-CoV-2 variants circulating in the
518 community (Crits-Christoph *et al.*, 2021; Jahn *et al.*, 2021). WBE for SARS-CoV-2, and
519 future emerging pathogens, has the potential to target the need for more localized
520 clinical testing, facilitating the detection of occasional hotspots of infection likely to
521 occur as this or other pandemics take place. It is scalable, with a fast turnaround, and
522 economically competitive. WBE could be useful in school or nursing home settings, to

523 evaluate the presence and spread of the viruses instead of testing hundreds or
524 thousands of individuals. Additionally, WBE can be a very powerful tool in countries
525 with limited resources, to inform decisions and in aiding with policy making.

526 4. Conclusion

- 527 • SARS-CoV-2 RNA was detected in raw wastewater of all five studied WWTP
528 at concentrations similar to those reported in other studies. Data reflected the
529 different epidemiological stages, including surges and decreases, observed
530 with the syndromic surveillance.
- 531 • The selection of sampling methods, composite vs grab, may have a massive
532 impact in the results and potential use of WBE for SARS-CoV-2 or any other
533 future pandemic, particularly in situations where low circulation of the
534 microorganism is expected.
- 535 • The total load of SARS-CoV-2 RNA in raw wastewater followed a similar trend
536 to the number of daily new COVID-19 reported cases. Considering data, the
537 use of viral loading would be a more suitable approach than gene-based
538 approaches to use in WBE settings. We consider using the number of daily new
539 COVID-19 reported cases a more suitable approach to simply comparing with
540 cumulative number of cases especially when dealing with several waves of
541 infection.
- 542 • Data from this study corroborates the plausibility and timeliness of the
543 development and deployment of a nationwide WBE system for SARS-CoV-2
544 (naturally, ideally scalable for future pandemics) to aid local health and
545 governmental authorities in policy making to help with future health crisis.

546

547 **Funding**

548 This work was supported by Programa Operacional de Competitividade e Internacionalização (POCI)
549 (FEDER component), Programa Operacional Regional de Lisboa, and Programa Operacional Regional
550 do Norte (Project COVIDTECT, ref. 048467).

551

552 **Declaration of Competing Interest**

553 The authors declare that they have no known competing financial interests or personal relationships
554 that could have appeared to influence the work reported in this paper.

555
556 **Acknowledgements**

557 We thank all the workers from Águas de Portugal Group who contributed to wastewater sampling. We
558 also thank the project's Advisory Board (EPAL, Águas do Douro e Paiva, National Environment Agency
559 (APA), National Health Authority (DGS) and Portuguese Water and Waste Services Regulation
560 Authority (ERSAR).

561 Strategic funding of Fundação para a Ciência e a Tecnologia (FCT), Portugal, to cE3c and BiolSI
562 Research Units (UIDB/00329/2020 and UIDB/04046/2020] is also gratefully acknowledged.

563 References

- 564 Ahmed, W., Bertsch, P.M., Bivins, A., Bibby, K., Farkas, K., Gathercole, A., Haramoto,
565 E., Gyawali, P., Korajkic, A., McMinn, B.R., Mueller, J.F., Simpson, S.L., Smith, W.J.,
566 Symonds, E.M., Thomas, K.V., Verhagen, R., Kitajima, M., 2020. Comparison of virus
567 concentration methods for the RT-qPCR-based recovery of murine hepatitis A virus,
568 a surrogate for SARS-CoV-2 from untreated wastewater. *Sci. Total Environ.* 739,
569 139960. doi: 10.1016/j.scitotenv.2020.139960
- 570 Baert, L., Wobus, C.E., Van Coillie, E., Thackray, L.B., Debevere, J., Uyttendaele, M.,
571 2008. Detection of Murine Norovirus 1 using plaque assay, transfection assay, and
572 real-time reverse-transcription-PCR before and after heat exposure. *Appl. Environ.*
573 *Microbiol.* 74 (2), 543-546. doi: 10.1128/AEM.01039-07
- 574 Baird, R.B., Eaton, A.D., Rice, E.W., 2017. *Standard Methods for the Examination of*
575 *Water and Wastewater*, 23rd ed. American Public Health Association, Washington DC.
- 576 Blanco, A., Abid, I., Al-Otaibi, N., Pérez-Rodríguez, F.J., Fuentes, C., Guix, S., Pintó,
577 R.M., Bosch, A., 2020. Glass wool concentration and optimization for the detection of
578 enveloped and non-enveloped waterborne viruses. *Food Environ. Virol.* 11 (2), 184-
579 192. doi: 10.1007/s12560-019-09378-0
- 580 Chavarria-Miró, G., Anfruns-Estrada, E., Guix, S., Paraira, M., Galofré, B., Sánchez,
581 G., Pintó, R., Bosch, A., 2020. Sentinel surveillance of SARS-CoV-2 in wastewater
582 anticipates the occurrence of COVID-19 cases. *medRxiv* doi:
583 10.1101/2020.06.13.20129627
- 584 Choi, P.M., Tschärke, B.J., Donner, E., O'Brien, J.W., Grant, S.C., Kaserzon, S.L.,
585 Mackie, R., O'Mally, E., Crosbie, N.D., Thomas, K.V., Mueller, J.F., 2018. Wastewater-
586 based epidemiology biomarkers: Past, present and future. *Trends Analyt. Chem.* 105,
587 453-469. doi: 10.1016/j.trac.2018.06.004

588 Corman, V.M., Landt, O., Kaiser, M., Molenkamp, R., Meijer, A., Chu, D.K.W.,
589 Bleicker, T., Brünink, S., Schneider, J., Schmidt, M.L., Mulders, D., Haagmans, B.L.,
590 van der Veer, B., van der Brink, S., Wijsman, L., Goderski, G., Romette, J.-L., Ellis, J.,
591 Zambon, M., Peiris, M., Goossens, H., Reusken, C., Koopmans, M., Drosten, C., 2020.
592 Detection of 2019 novel coronavirus (2019-nCoV) by real-time RT-PCR. *Euro Surveill.*
593 25 (3), 2000045. doi: 10.2807/1560-7917.ES.2020.25.3.2000045

594 Cornman, R.S., McKenna, J.E. Jr., Fike, J., Oyler-McCance, S.J., Johnson, R., 2018.
595 An experimental comparison of composite and grab sampling of stream water for
596 metagenetic analysis of environmental DNA. *PeerJ* 6:e5871. doi: 10.7717/peerj.5871

597 Crits-Christoph, A., Kantor, R.S., Olm, M.R., Whitney, O.N., Al-Shayeb, B., Lou, Y.C.,
598 Flamholz, A., Greenwald, H., Hinkle, A., Hetzel, J., Spitzer, S., Koble, J., Tan, A.,
599 Hyde, F., Schroth, G., Kuersten, S., Banfield, J.F., Nelson, K.L., 2021. Genome
600 sequencing of sewage detects regionally prevalent SARS-CoV-2 variants. *mBio* 12(1):
601 e02703-20. doi: 10.1128/mBio.02703-20

602 DGS, 2020. Novo Coronavírus – COVID-19: relatório da situação. [https://covid19.min-](https://covid19.min-saude.pt/relatorio-de-situacao/)
603 [saude.pt/relatorio-de-situacao/](https://covid19.min-saude.pt/relatorio-de-situacao/) (last accessed 10 March 2020).

604 EC, 2021. Commission Recommendation of 17.3.2021 on a common approach to
605 establish a systematic surveillance of SARS-CoV-2 and its variants in wastewater in
606 the EU. Brussels, Belgium.

607 Flood, M., D'Souza, N., Rose, J.B., Aw, T.G., 2021. Methods evaluation for rapid
608 concentration and quantification of SARS-CoV-2 in raw wastewater using droplet
609 digital and quantitative RT-PCR. *Food Environ. Virol.* 13, 303-315. doi:
610 10.1007/s12560-021-09488-8

611 Gonçalves, J., Koritnik, T., Mioč, V., Trkov, M., Bolješič, M., Berginc, N., Prosenc, K.,
612 Kotar, T., Paragi, M., 2021. Detection of SARS-CoV-2 RNA in hospital wastewater

613 from a low COVID-19 disease prevalence area. *Sci. Total Environ.* 755 (Part 2),
614 143226.

615 Gonzalez, R., Curtis, K., Bivins, A., Bibby, A., Weir, M.H., Yetka, K., Thompson, H.,
616 Keeling, D., Mitchell, J., Gonzalez, D., 2020. COVID-19 surveillance in Southeastern
617 Virginia using wastewater-based epidemiology. *Water Res.* 186, 116296. doi:
618 10.1016/j.watres.2020.116296

619 He, X., Lau, E.H.Y., Wu, P., Deng, X., Wang, J., Hao, X., Lau, Y.C., Wong, J.Y., Guan,
620 Y.G., Tan, X., Mo, X., Chen, Y., Liao, B., Chen, W., Hu, F., Zhang, Q., Zhong, M., Wu,
621 Y., Zhao, L. Zhang, F., Cowling, B.J., Li, F., Leung, G.M., 2020. Temporal dynamics
622 in viral shedding and transmissibility of COVID-19. *Nat. Med.* 26, 672-675. doi:
623 10.1038/s41591-020-0869-5

624 Hovi, T., Shulman, L.M., Van der Avoort, H., Deshpande, J., Roivainen, M., De
625 Gourville, E.M., 2012. Role of environmental poliovirus surveillance in global polio
626 eradication and beyond. *Epidemiol. Infect.* 140(1), 1-13. doi:
627 10.1017/s095026881000316x

628 Jahn, K., Dreifuss, D., Topolsky, I., Kull, A., Ganesanandamoorthy, P., Fernandez-
629 Cassi, X., Bänziger, C., Stachler, E., Furhmann, L., Jablonski, K.P., Chen, C., Aquino,
630 C., Stadler, T., Ort, C., Kohn, T., Julian, T.R., Beerenwinkel, N., 2021. Detection of
631 SARS-CoV-2 variants in Switzerland by genomic analysis of wastewater samples.
632 medRxiv. doi: 10.1101/2021.01.08.21249379

633 Jarvis, B., 2007. On the compositing of samples for qualitative microbiological testing.
634 *Lett. Appl. Microbiol.* 45, 592-598. doi: 10.1111/j.1472-765X.2007.02237.x

635 Koopmans, J.S., Henry, C.J., Park, J.H., Eisenberg, M.C., Ionides, E.L., Eisenberg,
636 J.N., 2017. Dynamics affecting the risk of silent circulation when oral polio vaccination
637 is stopped. *Epidemics* 20, 21-36. doi: 10.1016/j.epidem.2017.02.013

638 La Rosa, G., Muscillo, M., 2013. Molecular detection of viruses in water and sewage,
639 in: Cook, N. (Ed.), *Viruses in Food and Water: Risks, Surveillance and Control*.
640 Woodhead Publishing Limited. Cambridge, pp. 97-125.

641 Lescure, F.-X., Bouadma, L., Nguyen, D., Parisey, M., Wicky, P.-H., Behillil, S.,
642 Gaymard, A., Bouscambert-Duchamp, M., Donati, F., Le Hingrat, Q., Enouf, V.,
643 Houhou-Fidouh, N., Valette, M., Mailles, A., Lucet, J.-C., Mentre, F., Duval, X.,
644 Descamps, D., Malvy, D., Timsit, J.-F., Lina, B., van-der-Werf, S., Yazdanpanah, Y.,
645 2020. Clinical and virological data of the first cases of COVID-19 in Europe: a case
646 series. *Lancet Infect. Dis.* 20 (6), 697-706. doi: 10.1016/S1473-3099(20)30200-0

647 Mandi, K.D., Overhage, J.M., Wagner, M.W., Lober, W.B., Sebastiani, P., Mostashari,
648 F., Pavlin, J.A., Gesteland, P.H., Treadwell, T., Koski, E., Hutwagner, L., Buckeridge,
649 D.L., Aller, R.D., Grannis, S., 2004. Implementing syndromic surveillance: a practical
650 guide informed by the early experiences. *J. Am. Med. Inform. Assoc.* 11(2), 141-150.
651 doi: 10.1197/jamia.M1356

652 Medema, G., Heijnen, L., Elsinga, G., Italiaander, R., Brouwer, A., 2020. Presence of
653 SARS-Coronavirus-2 RNA in sewage and correlation with reported COVID-19
654 prevalence in the early stage of the epidemic in The Netherlands. *Environ. Sci.*
655 *Technol. Lett.* doi: 10.1021/acs.estlett.0c00357

656 Meselson, M., 2020. Droplets and aerosols in the transmission of SARS-CoV-2. *N.*
657 *Eng. J. Med.* 382(21), 2063. doi: 10.1056/NEJMc2009324

658 Pan, Y., Zhang, D., Yang, P., Poon, L.L.M., Wang, Q., 2020. Viral load of SARS-CoV-
659 2 in clinical samples. *Lancet Infect. Dis.* 20 (4), 411-412. doi: 10.1016/S1473-
660 3099(20)30113-4

661 Philo, S., Keim, E., Swanstrom, R., Ong, A., Burnor, E., Kossik, A., Harrison, J.,
662 Demeke, B., Zhou, N., Beck, N., Shirai, J., Meschke, J.S., 2020. A comparison of

663 SARS-CoV-2 wastewater concentration methods for environmental surveillance. *Sci.*
664 *Total. Environ.* 760:144215. doi: 10.1016/j.scitotenv.2020.144215.

665 Randazzo, W., Truchado, P., Ferranfo, E.C., Simon, P., Allende, A., Sanchez, G.,
666 2020. SARS-CoV-2 RNA titers in wastewater anticipated COVID-19 occurrence in a
667 low prevalence area. *Water Res.* 181, 115942. doi: 10.1016/j.watres.2020.115942

668 Reddy, D., 2010. Responding to pandemic (H1N1) 2009 influenza: the role of
669 oseltamivir. *J. Antimicrob. Chemother.* 65 (suppl. 2), ii35-ii40. doi: 10.1093/jac/dkq014.

670 RTP, 2020. 'COVID-19. Ministra admite que Portugal entra em "fase de crescimento
671 exponencial". [https://www.rtp.pt/noticias/mundo/covid-19-ministra-admite-que-](https://www.rtp.pt/noticias/mundo/covid-19-ministra-admite-que-portugal-entra-em-fase-de-crescimento-exponencial_e1212035)
672 [portugal-entra-em-fase-de-crescimento-exponencial_e1212035](https://www.rtp.pt/noticias/mundo/covid-19-ministra-admite-que-portugal-entra-em-fase-de-crescimento-exponencial_e1212035). Last accessed: 16
673 March 2021.

674 Santos, R., Monteiro, S., 2013. Epidemiology, control, and prevention of emerging
675 zoonotic viruses, in: Cook, N. (Ed.), *Viruses in Food and Water: Risks, Surveillance*
676 *and Control*. Woodhead Publishing Limited. Cambridge, pp. 442-457.

677 Sherchan, S.P., Shahin, S., Ward, L.M., Tandukar, S., Aw, T.G., Schmitz, B., Ahmed,
678 W., Kitajima, M., 2020. First detection of SARS-CoV-2 RNA in wastewater in North
679 America: a study in Louisiana, USA. *Sci. Total Environ.* 743, 140621. doi:
680 10.1016/j.scitotenv.2020.140621

681 Singer, A.C., Järhult, J.D., Grabic, R., Khan, G.A., Fedorova, G., Fick, J., Lindberg,
682 R.H., Bowes, M.J., Olsen, B., Söderström, H., 2013. Compliance to oseltamivir among
683 two populations in Oxfordshire, United Kingdom affected by influenza A(H1N1)pdm09,
684 November, 2009 – a waste water epidemiology study. *PLoS One* 8, e60221. doi:
685 10.1371/journal.pone.0060221

686 U.S. Geological Survey, 2006. *Techniques and methods 1-D3: guidelines and*
687 *standard procedures for continuous water-quality monitors: station operation, record*

688 computation, and data reporting. <https://pubs.usgs.gov/tm/2006/tm1D3/> (last
689 accessed 7 September 2020)

690 U.S. Geological Survey, 2010. Scientific investigations report 2010-5008: use of
691 continuous monitors and autosamples to predict unmeasured water-quality
692 constituents in tributaries of the Tualatin River, Oregon.
693 <https://pubs.usgs.gov/sir/2010/5008/lot.html> (last accessed 7 September 2020).

694 Wang, J. Feng, H., Zhang, S., Ni, Z., Ni, L., Chen, Y., Zhuo, L., Zhong, Z., Qu, T.,
695 2020. SARS-CoV-2 RNA detection of hospital isolation wards hygiene monitoring
696 during the Coronavirus Disease 2019 outbreak in a Chinese hospital. *Int. J. Inf. Dis.*
697 *94*, 103-106. doi: 10.1016/j.scitotenv.2020.139652

698 Westhaus, S., Weber, F.-A., Schiwy, S., Linnemann, V., Brinkmann, M., Widera, M.,
699 Greve, C., Janke, A., Hollert, H., Wintgens, T., Ciesek, S., 2020. Detection of SARS-
700 CoV-2 in raw and treated wastewater in Germany – Suitability for COVID-19
701 surveillance and potential transmission risks. *Sci. Total Environ.* *751*, 141750. doi:
702 10.1016/j.scitotenv.2020.141750

703 Wigginton, K.R., Ye, Y., Ellenberg, R.M., 2015. Emerging investigators series: the
704 source and fate of pandemic viruses in the urban water cycle. *Environ. Sci.: Water*
705 *Res. Technol.* *1*: 735.

706 Wölfel, R., Corman, V.M., Guggemos, W., Seilmaier, M., Zange, S., Müller, M.A.,
707 Niemeyer, D., Jones, T.C., Vollmar, P., Rothe, C., Hoelscher, M., Bleicker, T., Brünink,
708 S., Schneider, J., Ehmann, R., Zwirgmaier, K., Drosten, C., Wendtner, C., 2020.
709 Virological assessment of hospitalized patients with COVID-2019. *Nature* *581*, 465-
710 469. doi: 10.1038/s41586-020-2196-x

711 WHO, 2015. Guidelines on Environmental Surveillance for Detection of Polioviruses,
712 Working Draft. Geneva, Switzerland. [http://polioeradication.org/wp-](http://polioeradication.org/wp-content/uploads/2016/07/GPLN_GuidelinesES_April2015.pdf)
713 [content/uploads/2016/07/GPLN_GuidelinesES_April2015.pdf](http://polioeradication.org/wp-content/uploads/2016/07/GPLN_GuidelinesES_April2015.pdf)

714 Wu, F., Xiao, A., Zhang, J., Gu, X., Lee, W.L., Kauffman, K., Hanage, W., Matus, M.,
715 Ghaeli, N., Endo, N., Duvallet, C., Moniz, K., Erickson, T., Chai, P., Thompson, J.,
716 Alm, E., 2020. SARS-CoV-2 titers in wastewater are higher than expected from
717 clinically confirmed cases. MedRxiv doi: 10.1101/2020.04.05.20051540

718 Wu, Y., Guo, C., Tang, L., Hong, Z., Zhou, J., Dong, X., Yin, H., Xiao, Q., Tang, Y.,
719 Qu, X., Kuang, L., Fang, X., Mishra, N., Lu, J., Shan, H., Jiang, G., Huang, X., 2020.
720 Prolonged presence of SARS-CoV-2 viral RNA in faecal samples. Lancet
721 Gastroenterol. Hepatol. 5 (5), 434-435. doi: 10.1016/S2468-1253(20)30083-2

722 Wurtzer, S., Marechal, V., Mouchel, J.-M., Maday, Y., Teyssou, R., Richard, E.,
723 Almayrac, J.L., Moulin, L., 2020. Evaluation of lockdown effect on SARS-CoV-2
724 dynamics through viral genome quantification in waste water, Greater Paris, France,
725 5 March to 23 April 2020. Euro Surveill. 25: 2000776. doi: 10.2807/1560-
726 7917.ES.2020.25.50.2000776.

727 Xu, Y., Li, X., Zhu, B., Liang, H., Fang, C., Gong, Y., Guo, Q., Sun, X., Zhao, D., Shen,
728 J., Zhang, H., Liu, H., Xia, H., Tang, J., Zhang, K., Gong, S., 2020. Characteristics of
729 pediatric SARS-CoV-2 infection and potential evidence for persistent fecal viral
730 shedding. Nat. Med. 26 (4), 502-505. doi: 10.1038/s41591-020-0817-4

731 Young, B.E., Fong, S.-W., Chan, Y.-H. Mak, T.-M., Ang, L., Anderson, D., Lee, C.,
732 Amrun, S., Lee, B., Goh, Y., Su, Y., Wei, W., Kalimuddin, S., Chai, L., Pada, S., Tan,
733 S., Sun, L., Parthasarathy, P., Chen, Y., Barkham, T., Lin, R., Maurer-Stroh, S., Leo,
734 Y.-S., Wang, L.-F., Renia, L., Lee, V., Smith, G., Lye, D., Ng, L., 2020. Effect of a major
735 deletion in the SARS-CoV-2 genome on the severity of infection and the inflammatory

736 response: an observational cohort study. *The Lancet* 396(10251), 603-611. doi:
737 10.1016/S0140-6736(20)31757-8

738 Zang, R., Castro, M., McCune, B., Zeng, Q. Rothlauf, P., Sonnek, N., Liu, Z., Brulois,
739 K., Wang, X., Greenberg, H., Diamond, M., Ciorba, M., Whelan, S., Ding, S., 2020.
740 TMPRSS2 and TMPRSS4 promote SARS-CoV-2 infection of small intestinal
741 enterocytes. *Sci. Immunol.* 5(47), eabc3582. doi: 10.1126/sciimmunol.abc3582

742 Zhou, X., Zhang, T., Song, D., Huang, T., Peng, Q., Chen, Y., Li, A., Zhang, F., Wu,
743 Q., Ye, Y., Tang, Y., 2017. Comparison and evaluation of conventional RT-PCR SYBR
744 green I and TaqMan real-time RT-PCR assays for the detection of porcine epidemic
745 diarrhea virus. *Mol. Cell. Probes* 33, 36-41. doi: 10.1016/j.mcp.2017.02.002

746 Zuccato, E., Chiabrando, C., Castiglioni, S., Calamari, D., Bagnati, R., Schiarea, S.,
747 Fanelli, R., 2005. Cocaine in surface waters: a new evidence-based tool to monitor
748 community drug abuse. *Environ. Health* 4, 14. doi: 10.1186/1476-069X-4-14

749

Table 1.

Primers and probes used in this study

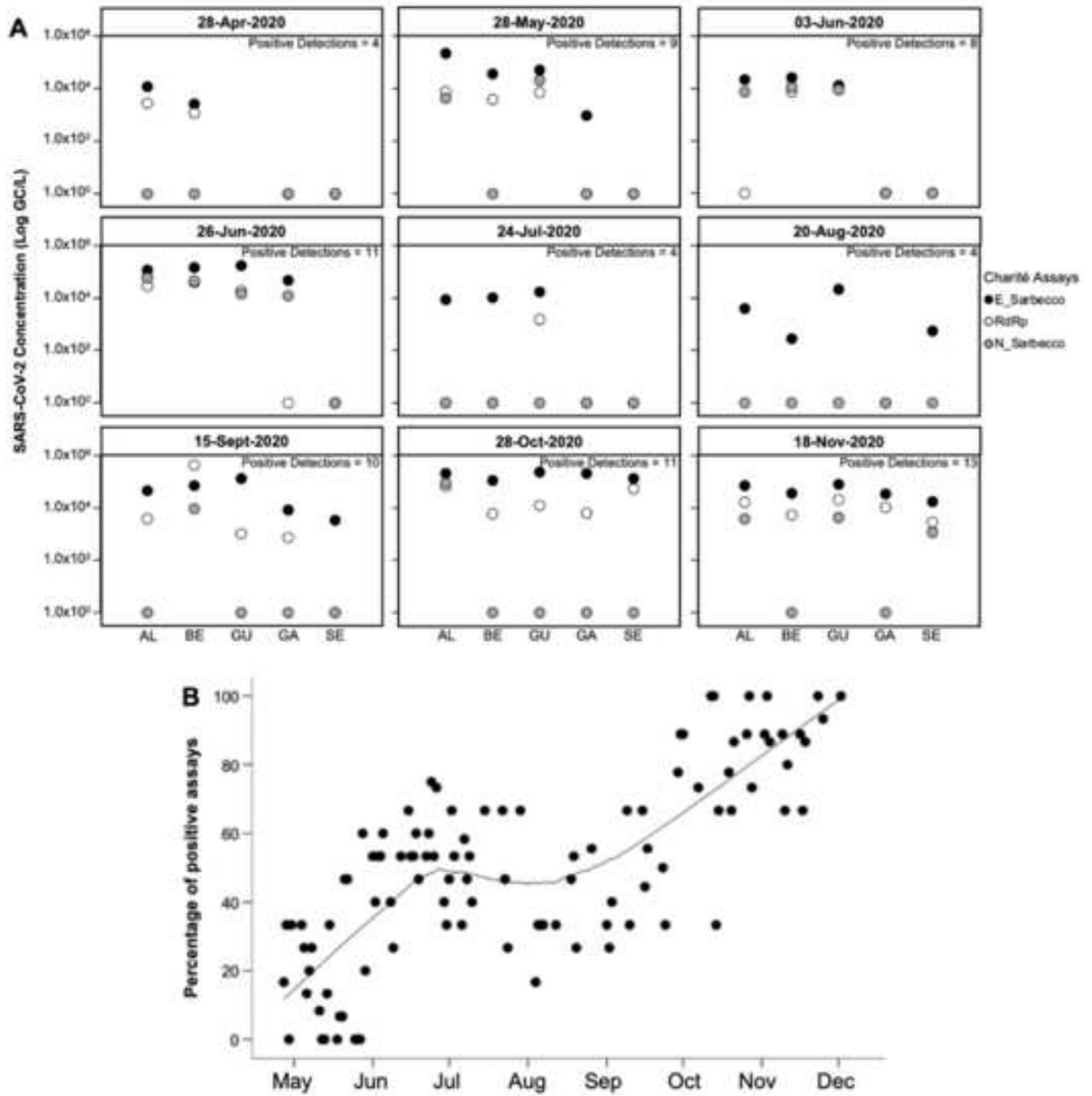
Assay	Sequence (5' - 3') ^a	Length (bp)	Location in SARS-CoV-2 genome (bp)
MNV	F: CACGCCACCGATCTGTTCTG R: GCGCTGCGCCATCACTC P: 6FAM-CGCTTTGGAACAATG-MGB	108	4,972 – 5,080
SARS-CoV-2: E_Sarbeco	F: ACAGGTACGTTAATAGTTAATAGCGT R: ATATTGCAGCAGTACGCACACA P: 6FAM-ACACTAGCCATCCTTACTGCGCTTCG-BHQ	112	26,141 – 26,253
SARS-CoV-2: RdRp	F: GTGARATGGTCATGTGTGGCGG R: CARATGTTAAASACACTATTAGCATA P1: 6FAM-CCAGGTGGWACRTCATCMGGTGATGC-BHQ P2: 6FAM-CAGGTGGAACCTCATCAGGAGATGC-BHQ	99	15,361 – 15,460
SARS-CoV-2: N_Sarbeco	F: CACATTGGCACCCGCAATC R: GAGGAACGAGAAGAGGCTTG P: 6FAM-ACTTCCTCAAGGAACAACATTGCCA-BHQ	127	28,555 – 28,682

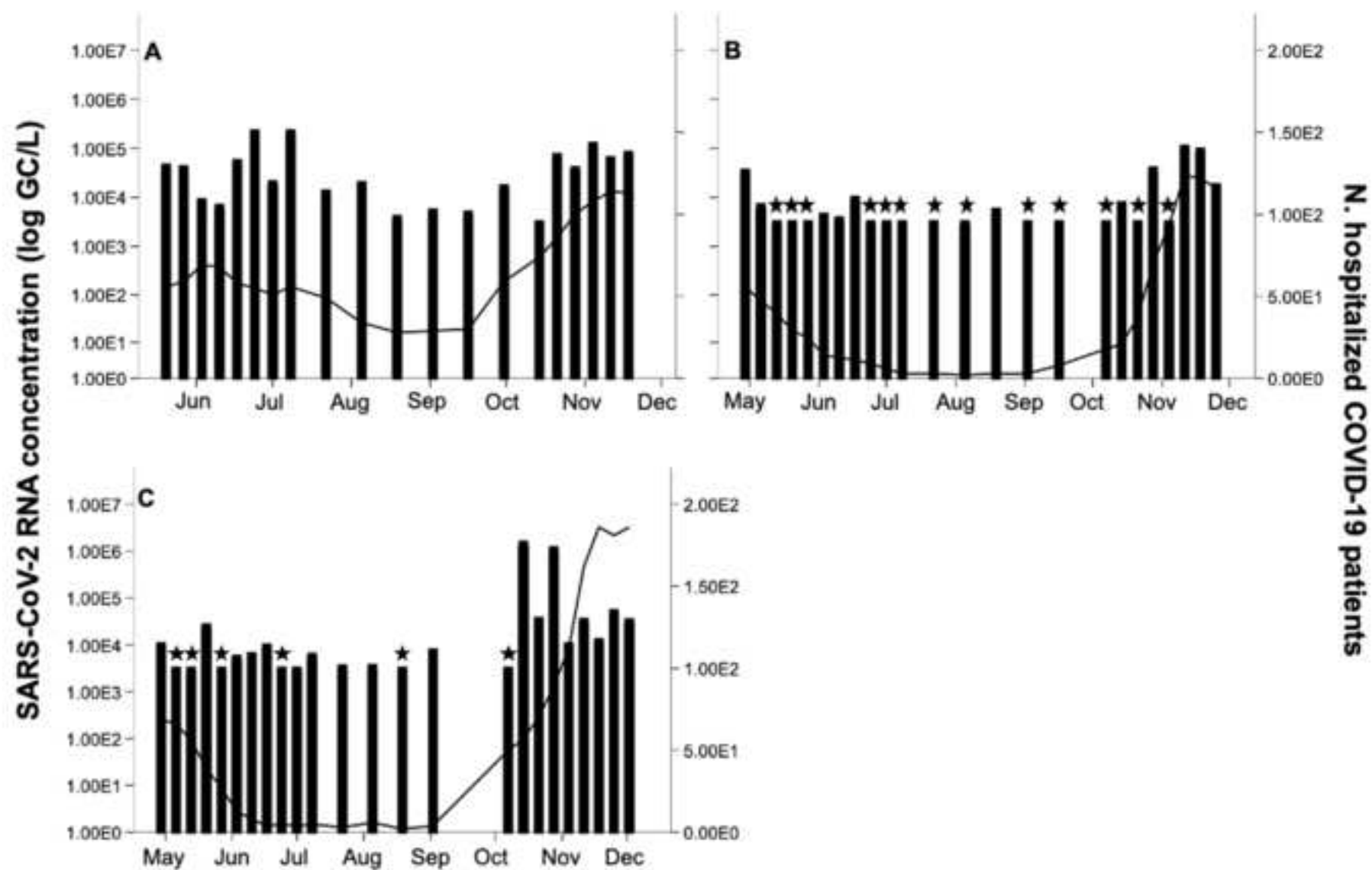
^a W is A/T; R is G/A; M is A/C; S is G/C. FAM: 6-carboxyfluorescein; MGB: minor groove binder; BHQ: blackhole quencher.

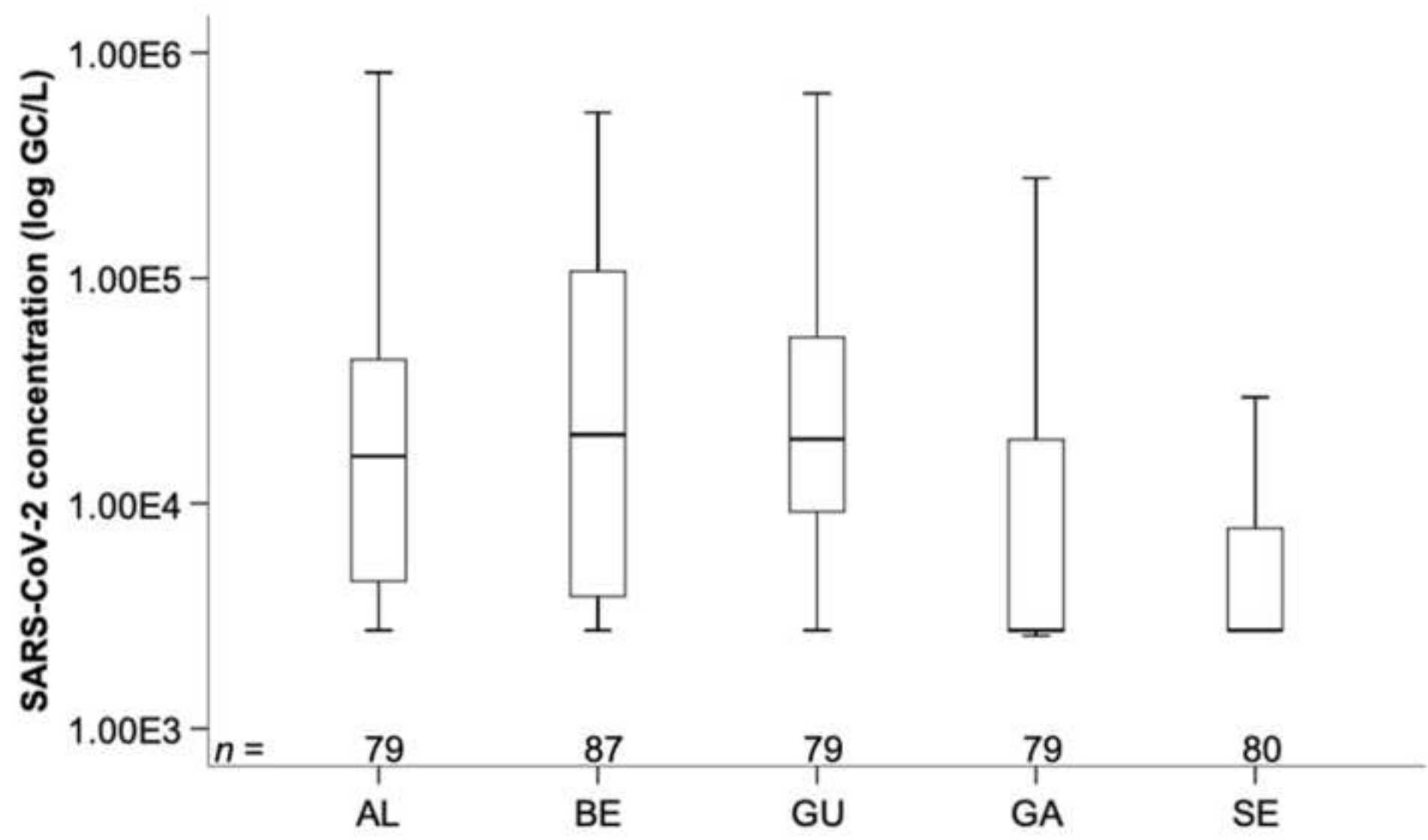
Table 2.

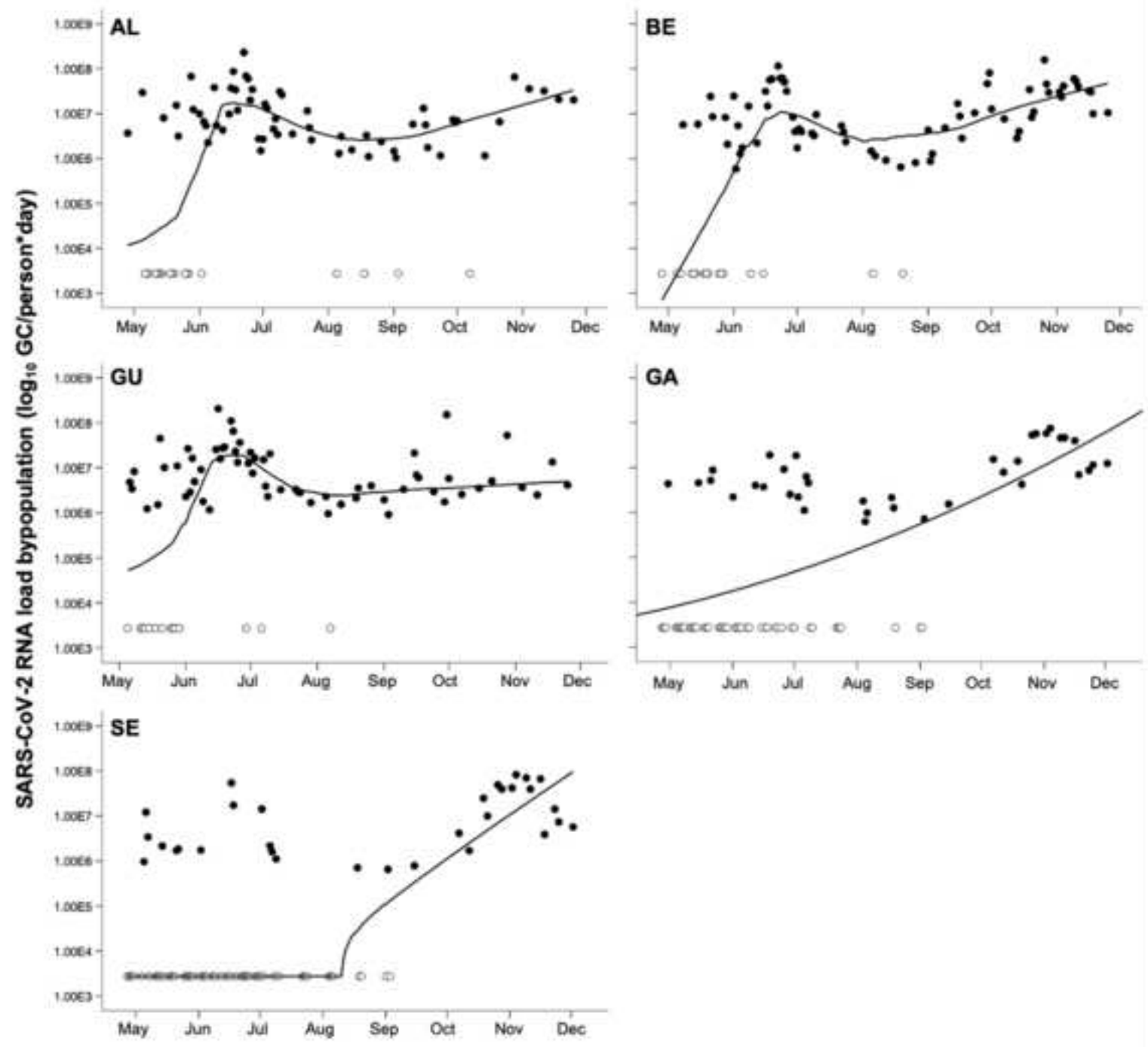
SARS-CoV-2 RNA concentration and percentage of positive samples in the overall study and in each WWTP

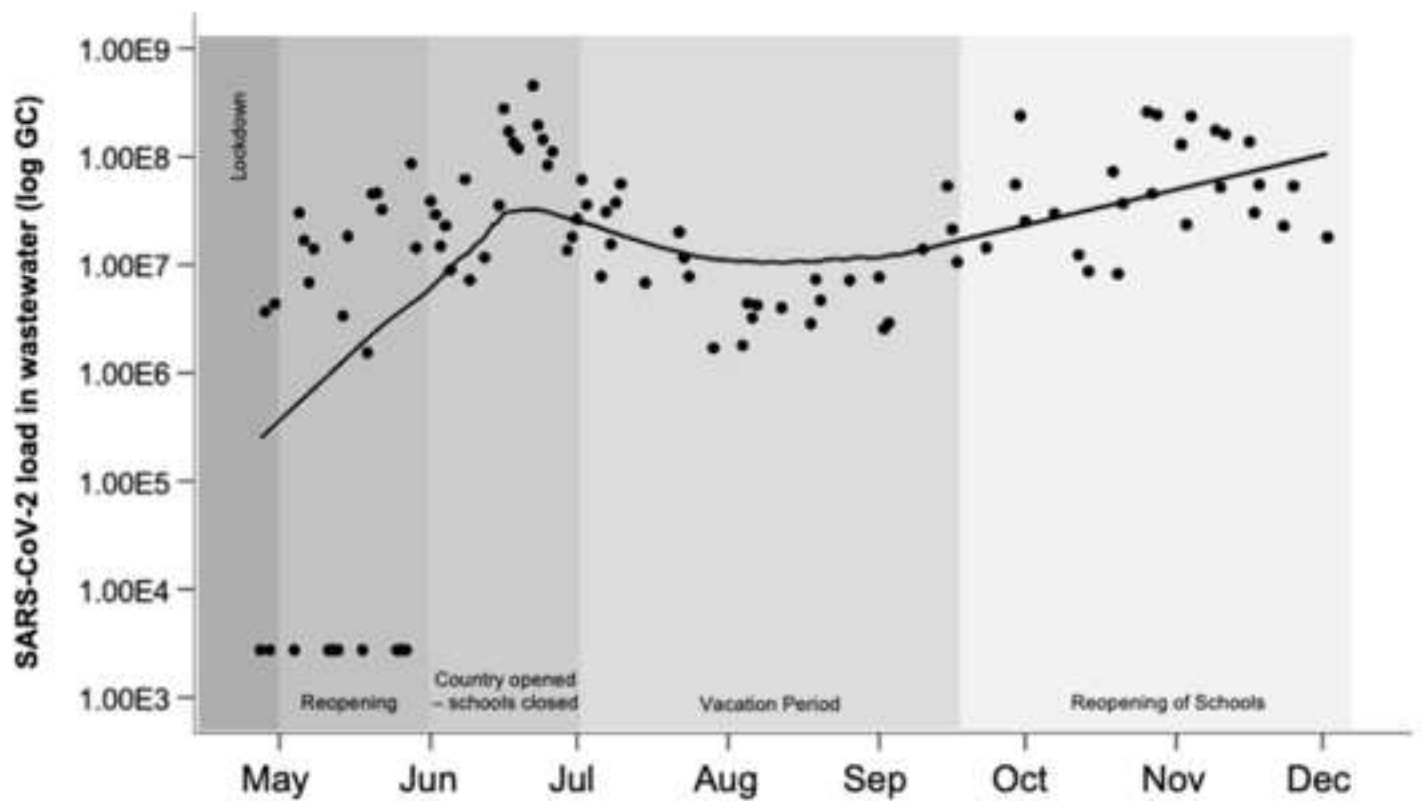
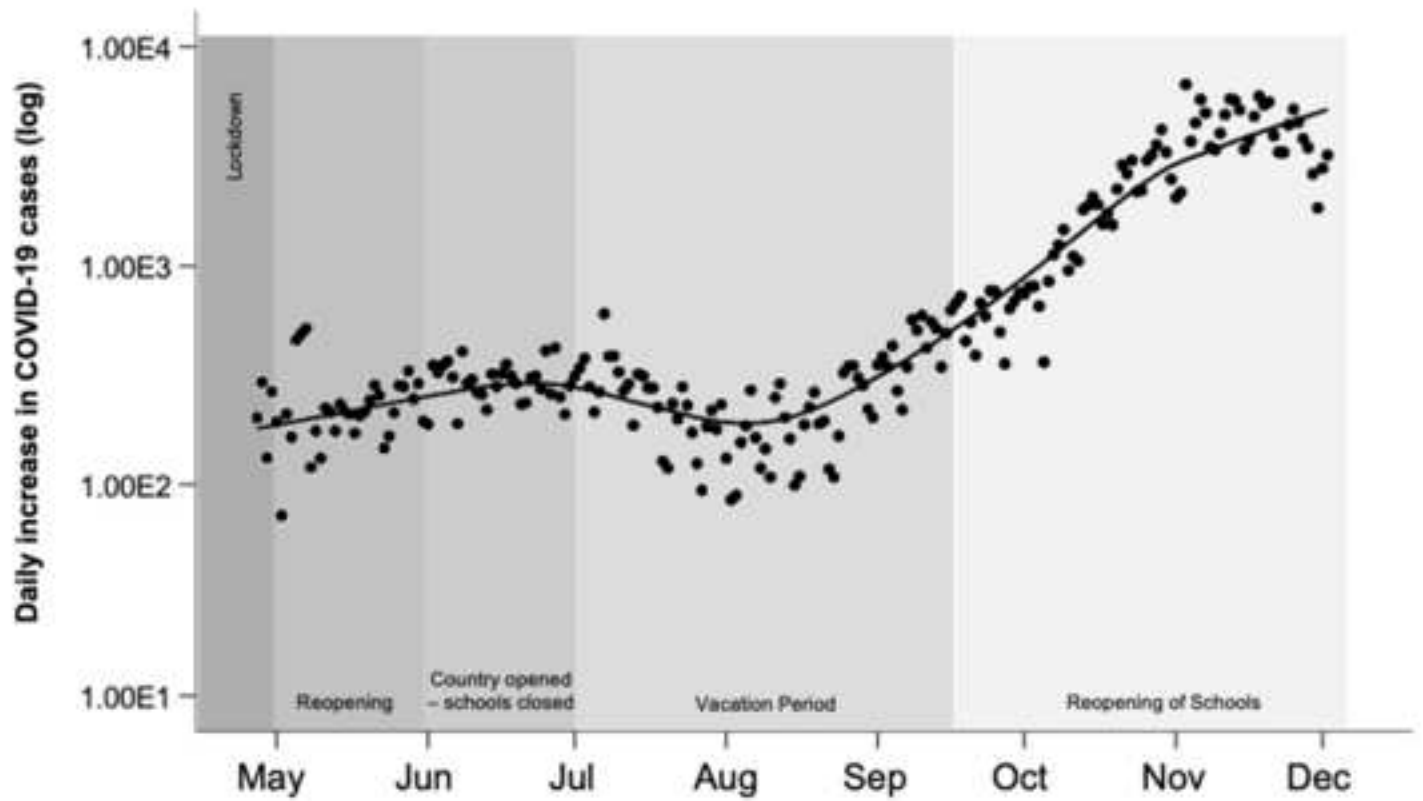
Sampling location	% Positive samples	SARS-CoV-2 RNA concentration variation (GC/L)
All WWTP	72 (291/404)	$3.13 \times 10^3 - 8.95 \times 10^5$
AL	82 (65/79)	$3.86 \times 10^3 - 8.17 \times 10^5$
BE	85 (74/87)	$3.13 \times 10^3 - 5.43 \times 10^5$
GU	85 (67/79)	$3.41 \times 10^3 - 8.95 \times 10^5$
GA	56 (44/79)	$3.30 \times 10^3 - 3.93 \times 10^5$
SE	51 (41/80)	$3.29 \times 10^3 - 3.20 \times 10^5$













[Click here to access/download](#)

Supplementary material for on-line publication only
Supplementary_Materials.docx



CrediT authorship contribution statement

Sílvia Monteiro: conceptualization, methodology, software, validation, formal analysis, investigation, writing – original draft, writing – review and editing, visualization. **Daniela Rente:** investigation. **Mónica V. Cunha:** review and editing. **Manuel Carmo Gomes:** review and editing. **Tiago A. Marques:** review and editing. **Artur B. Lourenço:** review and editing. **Eugénia Cardoso:** review and editing, sampling; **Pedro Álvaro:** review and editing, sampling; **João Vilaça:** review and editing, sampling; **Fátima Meireles:** review and editing, sampling; **Nuno Brôco:** project administration, funding acquisition, review and editing; **Marta Carvalho:** project administration, funding acquisition, review and editing; **Ricardo Santos:** conceptualization, methodology, resources, formal analysis, writing – review and editing.

Declaration of Competing Interest

The authors declare that they have no known competing financial interests or personal relationships that could have appeared to influence the work reported in this paper.